WireSculptor: Interactive Guided Bending Workflow for Novice-Friendly Wire Sculpture Fabrication

Runze Xue[1], Fei Yu[1], Baohang Zhou[1], Jialu Wang[1], Fan Zhong[1], Qiong Zeng[1], and Haisen Zhao[1]

Shandong University, 72 Binhai Highway, Qingdao, China
runzexue@outlook.com, maxmilitew@gmail.com, nychthelior@gmail.com,
jialuwang11@gmail.com, {zhongfan,qiong.zn,haisenzhao}@sdu.edu.cn

Abstract. This paper presents WireSculptor, an innovative interactive system designed to enable novices to create complex wire sculptures through an interactive guided bending workflow. In wire structure fabrication, manual bending offers flexibility in shaping intricate forms but is mainly suitable for experienced experts. To bridge this gap for novices, we construct a closed-loop guided bending workflow, which organically combines a visualization module for presenting precomputed bending instructions, and a bending error checker module for real-time error detection and feedback. To seek the most comfortable and effective bending setups for beginners, we apply a formative study on novices' bending operations, where we test different bending settings to see how they affect the forming quality and time novices take. Leveraging formative study findings, we craft bending instructions with a coarse-to-fine approach. First, users bend large-scale wire units segmented by bending points of salient curvature change. Following this, they make precise adjustments guided by instructions from a graph-cut-based line-circular segment fitting method. Technical evaluations demonstrate that most first-time users achieve higher accuracy when guided by our method compared to the unguided methods, all while preserving artistic expressiveness. Furthermore, several application areas have been explored in greater depth, namely artistic fonts, line art, and the physicalization of children's line drawing.

Keywords: Wire sculpture · wire fabrication · interactive guidance

1 Introduction

Wire sculpture involves crafting sculptures using wire, with roots in 2nd Dynasty Egypt and the Bronze and Iron Ages in Europe [27]. Today, wire sculpture remains of great significance in various modern contexts, spanning artistic creation, industrial design, handicraft education, and kinetic art installations [40]. While manual bending offers artistic flexibility for intricate wire shapes but challenges novices due to limited spatial cues, requiring substantial time and practice to
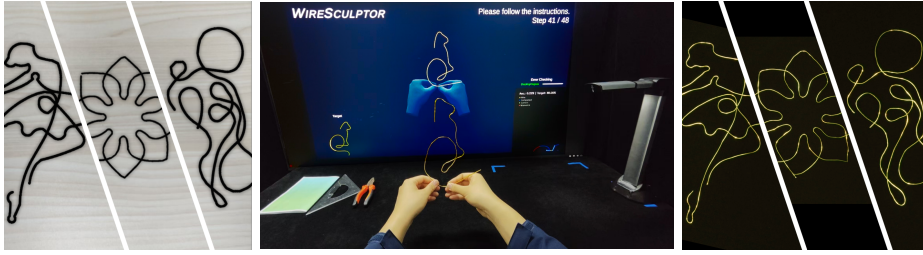
Fig. 1. For the input single-line wire sculptures (left), novice users utilize the proposed WireSculptor system to perform bending operations. The figure on the right demonstrates the resulting fabricated sculptures.

master [31]. Another potential challenge is that this manual process may be error-prone, discouraging artists, especially novices, to shape their ideas with the wire sculpturing. Conversely, automated machines bending offers high precision for industrial applications, it struggles to achieve the geometric complexity and artistic flexibility inherent in manual freehand bending [2]. Furthermore, hybrid approaches, like [41], integrates both strategies by adjusting the target shape to be collision-free for the wire bending machine and then having a human revert it to the target. However, such automated wire bending machines are not easy to afford for a novice users. This paper focuses on empowering *novices* to create wire sculptures with complex geometric features through manual bending. It aims to address the critical gap in guided workflows tailored to their needs in the specific applications. These applications range from creating prototypes of artistic fonts and line arts, to crafting Cloisonné works, and even physicalizing children's line drawings, as depicted in Figure 2.

The unique material characteristics of metal wire, including high elasticity and easy deformability, pose significant challenges for manual manipulation due to the inherent complexity and precision required [14]. Existing manual bending workflows rely heavily on expert intuition. Skilled practitioners optimize bending sequences by balancing global structural planning with local precision, leveraging years of experience for mature craftsmanship [13]. Novices, however, often lack such holistic understanding, resorting to trial-and-error approaches and various physical aids for manually aligning. These assistive tools may include 2D paper blueprints [43], or 3D-printed jigs that allow users to wind the wire into the preset cavity channels [19,32,31]. While these methods can enhance the rigid geometric accuracy of wire sculptures with relatively low geometric complexity, they still pose challenges when it comes to wire shapes with a lot of geometric details or many self-intersections [43]. This is because the physical assistance they provide becomes a limiting factor for novices, where it's hard for the novices to determine a feasible bending sequence. These methods fall short of offering clear, step-by-step guidance. As a result, novices lack support in crucial decision-making areas such as step sequencing and error rectification. Moreover, it is extremely

Fig. 2. Wire sculptures: Word art wire, 3D Ballerina art, parent-child activities, Cloisonne. [10,16,41].

challenging for novices to learn from a wire-bending expert, as such experts are rare and often difficult to access.

To tackle the issue of novice wire sculptors lacking sufficient guidance, we aim to further amplify guidance with a step-by-step visual instruction guided bending workflow for novices. As far as we know, the existing research work in this regard is still in its preliminary stage. Interactive guidance based on mixed reality [11] has proven transformative in domains like assembly tasks [37] and training for construction works [28] and team sports [6], yet remains scarcely explored for wire sculpture fabrication via bending operations [8]. We identified Dong et al . [8]'s study as the most relevant to our work, where they introduce ARAWTS, an AR-aided wire-bending training framework for orthodontics. It presents four standard training exercises and delivers feedback and improvement suggestions through gesture recognition [8]. However, ARAWTS is mainly oriented towards specific bending operations in orthodontic treatment and does not generate sequential guidance for arbitrary wire shapes.

To bridge this research gap of providing an interactive guided bending workflow, our key design philosophy prioritizes guiding novice operators through each step of the bending process. In this paper, we propose two fundamental bending operations: the *bend* operation for creating line segments and the *curve* operation for forming circular segments. To learn the novice users' technical limitations and preferences, we conduct a formative study to identify optimal bending configurations by examining how different parameters (such as the length of line segment, length of circular segment) influence both forming quality and operational efficiency. Building on these findings, we propose **WireSculptor**, a closed-loop guided bending workflow (illustrated in Figure 4), with the following key capabilities:

- a dual-scale decomposition approach using a coarse-to-fine strategy: the input wire is first divided at points of salient curvature change for users to shape large wire units; in the fine level, a graph-cut algorithm fits line-circular segments to assist users in refining wire bends accurately.
- a visualization module simultaneously presents wire deformation and hand-posture animations during each bending operation. These animations are rendered at a scale identical to the physical setup, ensuring accurate and intuitive guidance.

– a real-time quality detection module, highlighting inaccuracies in the wire with visual feedback to enable quick error identification and rectification. Additionally, it determines whether the user can advance to the next step based on the accuracy assessment.

Our main contribution is WireSculptor, the first guided bending workflow that empowers novices to fabricate intricate wire sculptures through step-by-step visual guidance and real-time error correction. Unlike traditional unguided approaches, in our experiment, we demonstrate its versatility through four application domains: artistic fonts, line art, wire-wrapped jewelry, and physicalized children's drawings. In the comparison, WireSculptor enables that most participants to bend wire sculptures with higher accuracy compared to two unguided approaches (static blueprints and jig-based assisted method). Furthermore, we demonstrate that WireSculptor is flexible to support diverse creative use cases, including artistic fonts, line art, and the physicalization of children's line drawing. WireSculptor's key contribution to HCI is demonstrating that an interactive guided strategy benefits novices in sculpture fabrication. Its system design also inspires other similar applications.

2   Related Work

2.1   Manual Wire Bending Techniques

Traditionally, manual wire bending has depended on skilled artisans' intuitive control of force and spatial reasoning [13], posing challenges for novices due to the absence of spatial and structural indicators [46]. To assist novices, researchers have developed various physical aids ranging from 2D templates [43] to 3D assistive devices, which are well designed for specific wire shapes and fabricated using 3D printing techniques. Garg et al. [15] create a 3D scaffold through laser cutting to assist the manual bending process of wire mesh. Iarussi et al. [19] produce physical jigs by extruding support walls from 2D jewelry drawings to guide wire wrapping operations. Torres et al. [32] propose ProxyPrint, a fabrication and construction proxy that enables a high-fidelity wire bending process. Wang et al. [29] propose FlexTruss with a construction pipeline to assemble truss-shaped objects by threading. [39] generate surface grooves on 3D models to serve as wire molds. More recently, Toji et al. [31] produce 3D-printed jigs for guiding the fabrication of multi-view wire art by humans.

While existing methods assist the manual bending process by providing spatial constraints, allowing novices to wrap wires around physical assistive devices, their utility diminishes significantly for complex shapes. As the target geometry grows intricate, these assistive structures themselves become increasingly elaborate, introducing new cognitive burdens: novices must not only navigate the device's physical complexity but also deduce operation sequences autonomously. Conversely, WireSculptor's intention is to assist novices at each step of the wire bending process.

2.2   Automated and Hybrid Bending Systems

In addition to manual methods, wire-bending machines for automatic bending [2], are extensively utilized in the industrial production of structural wire products. This includes elastically deforming wire structures that act as the skeletons for kinetic wire figures, as described in [42,24]. However, manufacturing most complex wire sculptures, especially those with many self-intersections, directly using wire bending machines poses challenges. Thus, the hybrid strategy combining machine and human wire bending techniques has been suggested: 1) a "decompose-then-assemble" strategy: first split the complex wire sculpture into fabricable sub-wires (planar rods [26] or Eulerian wires [23,3]), then manually assemble them into the final wire sculpture. 2) a "machine-then-human-bending" strategy with two bending stages is proposed in [41]. In the machine-bending stage, the wire bending machine realizes the deformed wire to ensure a collision-free CNC bending process. In the human-bending stage, with human assistance, the deformed wire is bent back to the target shape.

The mentioned automatic bending techniques produce rigid commands while considering the constraints of wire bending machines. Among the hybrid techniques featuring a manually-operated stage, there is a lack of step-by-step dynamic guidance during the human operation process. In contrast, WireSculptor guides novices through the bending steps, considering their skillset and preferences, where we perform an empirical study on novices' bending operations.

2.3   Guidance Assisted Fabrication

Guided workflows play a crucial role in enabling novices to acquire skills in the realm of crafts. Interactive guidance based on mixed reality [11] or online video parsing [37] has demonstrated its revolutionary impact in various fields, including, construction work training [28], team sports [6], rapid prototyping of breadboarded circuits [21], and active assembly [37,18]. For the design and fabrication of wire sculpture, mixed reality technologies have been applied. Examples include Pen2VR [22] and Y-AR [12], two mixed-reality systems for wire art design using a VR controller or hand gestures. WireDraw [46] is an augmented reality system for 3D wire object drawing with a 3D extruder pen. Except for ARAWTS [8], such interactive guidance techniques have rarely been applied to manual bending-based wire sculpture fabrication. ARAWTS uses AR to guide wire bending for dental applications, focusing on gesture recognition and error feedback. However, it is tailored to specific orthodontic wire types and lacks support to generate sequential guidance for arbitrary shapes. To address the above issue, we aim to further enhance the guidance through an interactive guided bending workflow tailored for novices.

2.4   Guidance Workflow Planning

This section presents related works on guidance fabrication workflow planning methods to assist human manual operation. Miguel et al. compute the stability-aware assembly sequence to assemble a set of planar-rod wire contours into a

single one [26]. Yu et al. propose LineUp, which generates a collision-free physical transformation motion to guide users in converting a single-line structure into a 3D model [45]. Liu et al. presents a motion planner algorithm for the robot arm to collaborate with a wire-bending machine to perform 3D metal wire curving [25]. Wang et al. propose an integrated design, simulation, and fabrication workflow for self-morphing electronics [38]. Yu et al. develop a process for crafting customizable interactive textiles [44]. For the guided bending workflow planning, Yang et al. [43] breaks a single-line 3D wire shape into near-planar segments, which can be printed into a set of blueprints to guide manual work. Wu et al. first decompose the input wire into a sequence of fabricable bending segments that comply with machine constraints [41], and then generate G-code bending commands for the wire-bending machine. During the manual bending stage, they do not provide specific instructions for users to bend the tuned points to the specified angles.

In conclusion, while prior work has explored manual aids and automated systems, no existing solution provides a closed-loop guided bending workflow that: 1) simplifies wire sculpture shapes into novice-friendly bending operations, 2) delivers sequential interactive guidance, and 3) provides real-time error correction. WireSculptor fills this research gap by combining algorithmic wire decomposition, interactive guidance of animated bending instructions, and feedback mechanisms, enabling novices to create intricate wire sculptures with unprecedented efficiency.

3   Design Exploration

Our core research question is how to design a wire sculpture system that effectively guides novice users in performing bending operations. To address this, we first summarize our design goals and then present our design framework.

3.1   Design Goals

The aim of wire sculpture guidance is to enhance novice users' quality and efficiency during the wire bending workflow. Based on literature review and informal semi-structured interviews with two artists, we identified three design goals:

- **D1. Provide novice-friendly instructions.** As our workflow is intended for novice users, the system should decompose complex wire sculpture designs into a sequence of simple, manageable steps. Each instruction should be easy to follow and executable with minimal prior experience or training. One of the artists we interviewed pointed out that "I can naturally come up with each subsequent step, but this might be hard for beginners." And another artist pointed out that "Novices often fail to organize global structural planning. But global structural planning remains critical for wire sculptures."
- **D2. Introduce step-by-step guidance via animations.** To help users stay aligned with the design intent and track their progress, the system

should incorporate animated visual guidance—such as illustrating the bending process—and highlight the correspondence between each bending operation and the intended target shape. One of the artists we interviewed pointed out that "Novices lack of the ability to observe." And another artist pointed out that "It would be beneficial for beginners to have mentor for teaching handcrafts step-by-step."

– **D3. Present intuitive quality evaluations**. The system should offer real-time, easy-to-understand feedback to help users detect and correct bending inaccuracies. For example, visual cues and performance metrics could be applied to guide users in refining their operations and improving overall fabrication quality. The artist pointed out that "I can't complete my handcrafts without iteratively tuning it according to the goal in my mind."

3.2   Design Framework

Motivated by the design goals identified above, we propose an interactive wire sculpture workflow specifically tailored for novice users. We structure the workflow design around four key aspects. First, we examine and explore fundamental parameter configurations in the human bending process. Next, we derive novice-friendly and executable fabrication instructions from a complex design. Following this, we identify the essential elements for effective guidance visualization and interactive feedback. Together, these components support novice users in sculpting wire structures step by step with improved accuracy and confidence.

Aspect 1: Human bending model. A core component of our workflow is a human bending model that captures how novice users perform wire bending under different bending configurations, which is essential for informing the design of fabrication instructions that are both executable and novice-friendly. To construct this model, we first conducted a formative study that systematically evaluated the effects of bending radius and angle on two key performance metrics: bending accuracy and time cost. By analyzing the collected data, we built predictive models that estimate user performance across various radius–angle combinations. These models are fundamental to generating novice-friendly instructions for fabrication steps that minimize error while maximize efficiency.

Aspect 2: Novice-friendly instructions. Novice-friendly instructions refer to a sequence of wire bending operations that are automatically translated from an input design. To generate these instructions, we adopt a dual-scale decomposition approach to divide the input wire, which transforms the original design into multi-level geometric primitives (coarse: large wire units; fine: line-circular segments), enabling a quick coarse-to-fine bending operation.

Aspect 3: Augmented guidance. Augmented visualization provides intuitive, real-time guidance by overlaying key cues—such as bend angles, directions, and sequence—onto a 3D virtual wire model. This visualization module guides novices through the fabrication process by presenting precomputed bending instructions

in an interactive and spatially meaningful way. Users align their physical operations with the animated guide, which serves as a dynamic scaffold that supports step-by-step execution.

Aspect 4: Intuitive feedback. Timely feedback is critical for preventing error accumulation during step-by-step wire fabrication. To address this need, we introduce a bending quality detection module that provides real-time error detection and corrective feedback. This lightweight mechanism continuously monitors deviations between the user's current bending result and the ground-truth geometry. When discrepancies are detected, the system issues intuitive alerts through color-coded visual overlays and concise textual prompts. These feedback cues help users quickly identify and correct errors.

4   Human Bending Model

(a) Web-based   (b) Photographic   (c) Error Rates Heatmap   (d) Time Cost Heatmap
    Interface   Apparatus   The lower the better.   The lower the better.
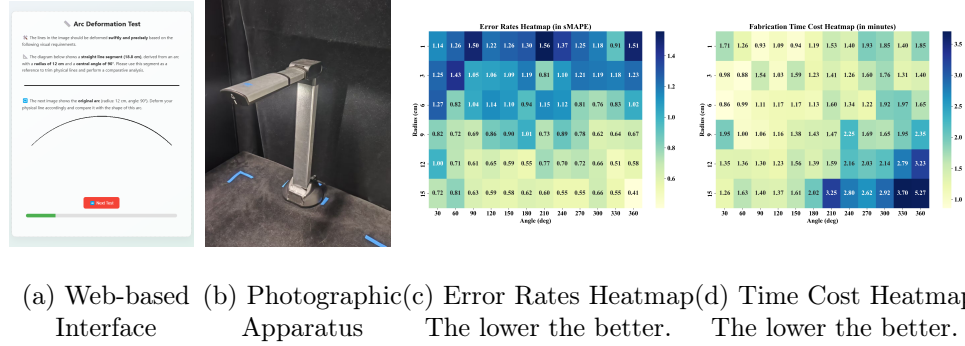
Fig. 3. An overview of the setups and results of our formative study. (a) The web-based interface to provide instructions for participants, with an example stimulus. (b) The high-speed photographic apparatus we used to capture the manually-bent curves. (c) - (d) The results of our formative study. Results demonstrate that larger radius and angle lead to lower error rates, while ultimate radius ($\geq$ 12 cm) and angle ($\geq$ 180°) lead to sharp increase in the fabrication time cost.

We aim to construct a human bending model that can identify optimal bending configurations for achieving high-quality and high-efficiency, novice-friendly operations. To this end, we first explore the research question: *how the accuracy and time cost for novice users to bend a simple wire segment under different bending radii and angles?* This question guided the design of a formative study to collect bending data from human subjects and to build a fitting model that interpolates between the tested values, enabling generalization across different combinations of bending radii and angles.

Table 1. The analysis result of the effects of bending radius and angle on error rates and time cost, using the ANOVA method. All P values < 0.05, indicating that both bending radius and angle show significant effects on both error rates and time cost. *: $p < 0.05$, **: $p < 0.01$, ***: $p < 0.001$.

Factor	Error Rates		Time	
	F	p	F	p
Radius	152.85	***	127.11	***
Angle	4.97	*	168.94	***

4.1 Formative Study

We conducted a formative study using a two-factor mixed design to examine the effects of bending radii and angles on the error rates and time costs of human bending operations. The two factors in the study are bending radius and bending angle, with a between-subjects design for bending radius and a within-subjects design for bending angle. Participants were required to bend a straight wire according to specific bending radii and angles. To mitigate learning effects, the presentation order of stimuli was randomized. The primary dependent variables were the quality of the bent wire, measured as the symmetric mean absolute percentage error (sMAPE) and the corresponding ground truth arc curves, and the time cost of the bending operation.

Stimuli. To simplify the bending curve and facilitate analysis, we generated a set of arc curves with varying bending radii and angles. Specifically, we defined the bending radius as the curvature radius of the arc, which was set to 1 and $3 \times n$ ($n = 1, 2, ..., 5$), with the unit of centimeters. We measured the bending angle using the central angle of the arc, which was set to values $30 \times m$ ($m = 1, 2, \cdots, 12$) with the unit of degree. In total, we generated a dataset of 72 unique visual stimuli. An example of our stimulus, along with the study interface, is shown in Figure 3 (a).

Participants. We recruited 24 participants with no prior experience in wire sculpture from the local university, majoring in computer science, law, economics, cryptography, and electric engineering. The sample size was determined based on an anticipated effect size of 0.8 and a statistical power of 0.7, equal to the minimum requirement of 12 participants (2 groups $\times$ 12 participants). Participant demographics included 17 males and 7 females, aged 18 to 25 years. Each participant was compensated approximately 10.32 dollars for their time, with an average task completion time of 75 minutes.

Tasks. Each participant was required to bend lines to replicate the shape of an arc curve displayed on the screen as accurately and quickly as possible. For each trial, we recorded the participant's bent curve along with the time taken to complete the task. The manually bent curves were captured using a high-speed photographic apparatus (see Figure 3 (b)).

Procedure. The experiment consisted of three phases. Participants began with a training phase involving three trials. They then proceeded to the line bending phase, which consisted of 36 trials, with a five-minute rest after completing the first 18 trials. After each trial, participants were required to place their bent curve under the photographic apparatus and capture a photo. The stimuli were randomized to minimize ordering and learning effects. Finally, participants completed a demographic information questionnaire. All phases of the experiment were conducted in a controlled, well-lit room, with participants seated approximately 55 cm from a screen with a resolution of 3840×1080 pixels.

Collected Data. We retained all data from the participants, resulting in a total of 864 trials. For each combination of bending radius and angle in a trial, we computed the sMAPE and time cost for each participant. Results are shown in Figure 3 (c)-(d).
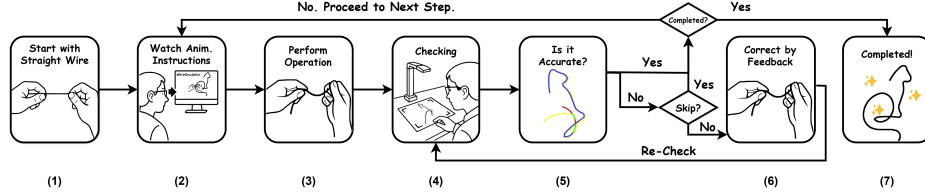

Fig. 4. The overview of our workflow. By watching the animated visualization and follow the instructions (2), the user perform operation (3) to deform the wire in order to fabricate the wire sculpture (7). Along with this process, the real-time error checker with feedback enables the user to make corrections (4) - (6).

4.2   Analysis & Model Construction

Based on the collected data from the user study, we first analyzed the impact of bending radius and angle on error rates and time costs during the bending process, using the ANOVA method. As shown in Table 1, we found significant effects of bending radius and angle on both error rates and time costs.

To construct the human bending models, we begin with two radius–angle metric tables representing error rates and time costs for specific combinations of radius r and angle θ, denoted as $T_e(r, \theta)$ and $T_t(r, \theta)$, respectively. In both tables, rows correspond to bending radii, columns correspond to bending angles, and each cell contains the average sMAPE in T_e or average time costs in T_t. Figure 3 (b) presents the averaged error rates (denoted as sMAPE) and time costs. We model both the error rates and time costs for an arbitrary combination of radius and angle using bilinear interpolation [7], which preserves trends and captures smooth transitions across radius-angle values and supports estimation for general combinations.

4.3   Findings

Overall, our results show statistically significant impacts of both bending radii and angles on both error rates and time costs during the bending processes. Based on our statistical analysis and models, we summarize the key findings of the human bending model:

 – **Effect of bending radius.** Error rates decrease as the bending radius increases. Sharper curves (i.e., smaller radii) introduce greater difficulty for novice users, resulting in higher error rates.
 – **Effect of bending angle.** Error rates decrease as the bending angle increases. However, when the bending radius ≥ 12 cm and the bending angle beyond $180°$, the fabrication time cost will sharply increase as the angle increases, where the bending path becomes substantially longer. We find that moderate angles ($60° \sim 120°$) tend to yield lower error rates without causing significant time costs.
 – **Novice-friendly design.** We recommend avoiding combinations of small radii and large angles when designing novice-friendly tasks. Wire sculptures can be optimized with radii larger than 6 cm and angles smaller than $120°$ to maximize accuracy and efficiency.

5   Wire Sculptor

5.1   Workflow Overview

We first provide an overview of the proposed interactive guided bending workflow, which is illustrated in Figure 4. Given a wire fabrication task, the system first coarsely decomposes the wire design into salient structural units, then finely fits each unit with simple line-circular segments, thus generating novice-friendly instructions with human bending model (Section 4) accordingly. Thereafter, animated visualization guides novices through the fabrication process by presenting these instructions. Along with this process, interactive real-time error checking and feedback are provided.

From the user's perspective, in one fabrication task, the user gradually deforms a straight wire into the final desired sculpture by repeating the following closed-loop steps:

 1. The user starts with a straight piece of wire (Figure 4 (1)).
 2. The user watches an animated novice-friendly instruction that demonstrates how to perform a small, localized fabrication operation (Figure 4 (2)).
 3. The user then freely performs the operation using any tools or hand techniques they prefer (Figure 4 (3)).
 4. At any time during or after the operation, the user can place the wire under the high-speed photographic apparatus to receive feedback (Figure 4 (4)).
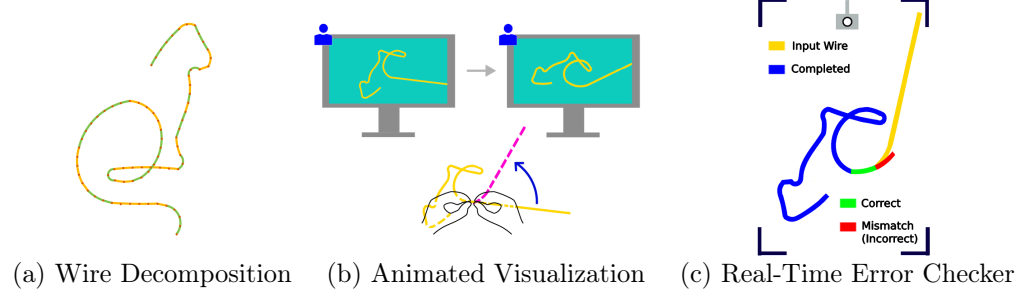 5. The workflow automatically checks the accuracy of the current progress (Figure 4 (5)).

(a) Wire Decomposition   (b) Animated Visualization   (c) Real-Time Error Checker

Fig. 5. The overview of our modules. Given an wire design as input, we first divide it into a coarse-to-fine bending segments (a). Subsequently, we generate an animated visualization guide for each fabrication step for guidance, demonstrating the operations required (b). Within each operation, an error checker (d) is utilized to check the current progress and provide visual feedback by highlighting inaccuracies.

    (a) If the progress is sufficiently accurate, the workflow proceeds to the next step (proceeding to step (2)), or reports that all instructions are finished (proceeding to step (7)).

    (b) If inaccuracies are detected, the system highlights the inaccurate regions in an overlaid image, enabling users to easily identify and rectify the issues, then the workflow proceeds to step (6). Alternatively, the user could interactively skip to next step (proceeding to step (2)).

6. The user freely correct the wire sculpture based on the highlighted inaccurate region. At any point during the correction process, the workflow can transition to step (4).

7. If all instructions are finished, the overall fabrication is completed.

We propose three central modules that collaboratively drive the *WireSculptor* workflow, enabling a guided fabrication experience, as shown in Figure 5:

– **Wire Decomposition**. This module includes a dual-scale decomposition approach to divide the input wire into coarse-to-fine bending segments, enabling generation of structured wire bending instructions.

– **Animated Visualization**. For each step, we generate an animated guide that visually demonstrates the operation required, aiding user comprehension and execution.

– **Real-Time Error Checker**. Within each operation, the system captures images of the current progress and evaluates its alignment with the target, offering visual feedback to assist users in correction.

5.2   Module 1: Wire Decomposition

This module decomposes complex wire designs in a coarse-to-fine manner, serving as a basis for generating animated wire bending instructions in Section 5.3. It employs a dual-scale decomposition approach. Given an input wire design, the
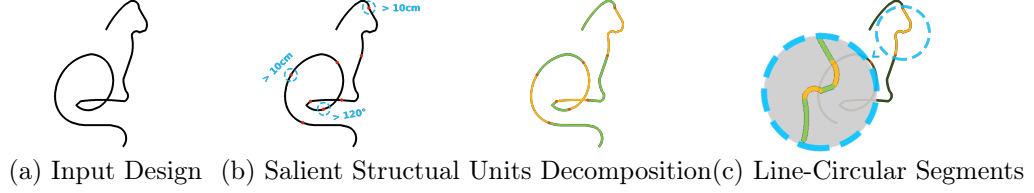
(a) Input Design (b) Salient Structual Units Decomposition(c) Line-Circular Segments

Fig. 6. The process of our dual-scale wire decomposition. Given a vector graphic as input design (a), we first decompose it into salient structural units (b) - (c). Thereafter, for each unit, we fit it with simple line-circular segments (d). These line-circular segments and units will be utilized in the generation of animated visualization.

dual-scale decomposition approach first decompose it into several salient structural units $\{U_0, U_1, \cdots\}$, and subsequently fit each unit U_i with a sequence of simple line-circular segments $S^{\text{final}} = \{s_0{}^{\text{final}}, s_1{}^{\text{final}}, \cdots\}$. As illustrated in Figure 6, this dual-scale decomposition approach involves *coarse-level: unit wire decomposition* and *fine-level: graph-cut-based segment fitting*.

Coarse-level: Unit Wire Decomposition Given a vector graphic of the wire design as input, the dual-scale decomposition approach aims to divide it into a sequence of units $\{U_0, U_1, \cdots\}$ at points of salient curvature change for users to shape large wire units. First, uniformly sample a sequence of points along the input wire. Then, compute the tangent line at each sampling point, which can be readily converted into a planar angle between the tangent line and the coordinate axis. Starting from one end of these sampling points, a traversal process is executed along the wire to generate each segment U_i with two criteria: 1) a total length is less than 10 cm or 2) the cumulative amount of planar angle change is less than $120°$.

Fine-level: Graph-Cut-Based Segment Fitting At the fine level, each unit is broken down into line-circular segments to assist users in applying the bending operations and to refine wire bends accurately. We adapt a graph-cut based segment fitting technique originally proposed in [41] for a wire bending machine. This adaptation is feasible because, as shown in [2], the interpolated bending strategy can realize line-segments, and the strike bending strategy can realize circular segments. These two types of bending segments are also essential for novice users. The graph-cut based segment fitting technique starts with generating candidate line-circular segments from each sampling point of a single line curve through a *forward-and-backward traverse* and a line-circular fitting procedure; these produced line-circular segments often overlap, so a graph-cut decomposition helps resolve the overlaps.

In our case, we generate candidate line-circular segments $S^{\text{cand}} = \{s_0{}^{\text{cand}}, s_1{}^{\text{cand}}, \cdots\}$ similarly but make a key change in the second step for resolving overlaps, with the consideration of these findings from Section 4. For each unit U_i, we construct a graph $G = (V, E, L)$. Assuming that the unit U_i contains $n + 2$ sampling points $P = \{p_0, p_1, \cdots, p_{n+1}\}$, the vertex set V represents a segment set

$S^{\text{init}} = \{s_0{}^{\text{init}}, s_1{}^{\text{init}}, \cdots, s_n{}^{\text{init}}\}$, where for each segment $s_i{}^{\text{init}}$, it linearly connects two adjacent points p_i, p_{i+1}. The edge set E is the sampling points P, where each $p_i \in P$ connects segments $s_i{}^{\text{init}}$ and $s_{i+1}{}^{\text{init}} \in S^{\text{init}}$, we aim to allocate a candidate line-circular segment $l_i = s_j{}^{\text{cand}}$ as its label. Our goal is to find an allocation $L = \{l_0, \cdots, l_n\}$ that minimizes the loss term $\mathcal{L}$, which is defined by:

$$\mathcal{L} = \sum_{i=0}^{n} \mathcal{L}_{\text{d}}(s_i{}^{\text{init}}, l_i) + \sum_{i=0}^{n-1} \mathcal{L}_{\text{sm}}(l_i, l_{i+1}) + \mathcal{L}_{\min}(L). \tag{1}$$

$\mathcal{L}_{\text{d}}$ denotes the data term measuring the cost of allocating l_i for $s_i{}^{\text{init}}$ and is defined by:

$$\mathcal{L}_{\text{d}}(s_i{}^{\text{init}}, l_i) = \begin{cases} \lambda_1 \cdot \mathcal{E}\left(l_i; \{s_i{}^{\text{init}}\}\right) \cdot \left(1 + \frac{e(l_i)}{2}\right)^{\lambda_2} & s_i{}^{\text{init}} \text{ in } l_i \\ \infty & \text{otherwise} \end{cases}, \tag{2}$$

where $\mathcal{E}$ denotes the maximum Euclidean distance between l_i and all $s_i{}^{\text{init}}$ covered. λ_1, λ_2 are hyper-parameters, and e denotes the difficulty of novice fabrication, which is calculated via interpolation on a lookup table filled with our formative study data. $e(l_i)$ is defined by:

$$e(l_i) = \begin{cases} \text{interp}\left(T_e; r(l_i), \theta(l_i)\right) & l_i \text{ is a circular segment} \\ 0 & \text{otherwise} \end{cases}, \tag{3}$$

where $r(l_i), \theta(l_i)$ denote the curvature radius and angle of the circular segment l_i, and $\text{interp}\left(T_e; r(l_i), \theta(l_i)\right)$ is calculated via bilinear interpolation on the error rate metric table T_e (see in Section 4.2).

$\mathcal{L}_{\text{sm}}$ denotes the smoothness term measuring the cost of allocating different labels (candidate segments $s_j{}^{\text{cand}}$) for the adjacent vertices $s_i{}^{\text{init}}, s_{i+1}{}^{\text{init}}$ and $\mathcal{L}_{\text{sm}}(l_i, l_{i+1})$ is set to 1 if $l_i \neq l_{i+1}$, otherwise, it's set to 0.

$\mathcal{L}_{\min}$ is utilized to minimize the number of final segments and is defined by:

$$\mathcal{L}_{\min}(L) = \sum_{s_i{}^{\text{cand}} \in S^{\text{cand}} \wedge s_i{}^{\text{cand}} \text{ occurs in } L} \lambda_3 t(s_i{}^{\text{cand}}), \tag{4}$$

where λ_3 is one hyper-parameter, and $t(s_i{}^{\text{cand}})$ is defined by:

$$t(s_i{}^{\text{cand}}) = \begin{cases} \text{interp}\left(T_t; r(s_i{}^{\text{cand}}), \theta(s_i{}^{\text{cand}})\right) & s_i{}^{\text{cand}} \text{ is a circular segment} \\ 0 & \text{otherwise} \end{cases}, \tag{5}$$

where $r(s_i{}^{\text{cand}}), \theta(s_i{}^{\text{cand}})$ denote the curvature radius and angle of the segment $s_i{}^{\text{cand}}$, and $\text{interp}\left(T_t; r(s_i{}^{\text{cand}}), \theta(s_i{}^{\text{cand}})\right)$ is calculated via bilinear interpolation on the time cost metric table T_t (see in Section 4.2).

By finding the allocation L that minimizes the loss term $\mathcal{L}$, we resolve overlaps with the consideration from Section 4. The final fine-level wire segments $S^{\text{final}} = \{s_0{}^{\text{final}}, s_1{}^{\text{final}}, \cdots\}$ that fit the unit U_i can be obtained then by removing duplicate elements from L. S^{final} will be utilized in the generation of animated visualization.

5.3   Module 2: Animated Visualization

The animated visualization module is engineered to create novice-friendly bending instructions, offering visual guidance to inexperienced users during the bending process. This is accomplished by transforming the decomposed dual-scale segments: the coarse-level structural wire segments $\{U_0, U_1, \cdots\}$ and the fine-level wire segments $S^{\mathrm{final}} = \{s_0^{\mathrm{final}}, s_1^{\mathrm{final}}, \cdots\}$ into animated instructions, as illustrated in Figure 8. To balance fabrication simplicity with shape fidelity, users are not prompted to start bending immediately after one animation of each individual fine-level line-circular segment; instead, animations are grouped based on coarse-level decomposition. All fine-level animations within each unit U_i are played in sequence, and then users perform the bending operations following the entire set of animations in that group.

(a) Start   (b) Process   (c) End
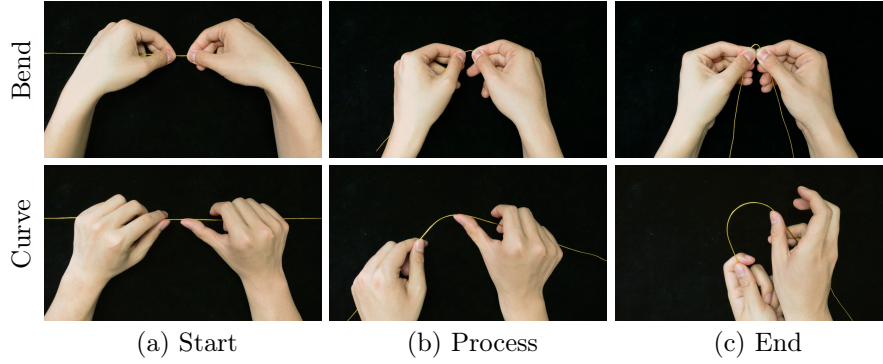
Fig. 7.   Illustrations of our two atomic bending operations. With bend or curve operations (a) - (b), novices can easily and conveniently fabricate nice-looking line or circular segments (c).

Therefore, the key technical challenges to realize the animated visualization module are twofold: 1) Determining the appropriate bending operations for the two types of fine-level segments (line segment and circular segment); 2) Developing a method to generate animated instructions that effectively visualize these bending operations.

Determining bending operations To address the first technical challenge, we introduce two fundamental fabrication operations (atomic bending operations): the **bend** operation for creating **line segments** and the **curve** operation for forming **circular segments**, illustrated in Figure 7.

- In the **bend** operation, the user exerts force at a pre-determined bending point on the wire, resulting in the wire folding at a particular angle.
- In the **curve** operation, the user gradually applies a uniform bending force along a section of the wire, thereby shaping it into a circular arc with the desired curvature.

Generating animated visualization To address the second challenge of generating animated visualization instructions for these atomic bending operations, we generate wire deformation animations to illustrate the wire's deformation procedure, and hand-gesture animations to demonstrate how the designated segment should be manipulated by hands, implemented with the Unity Engine [33].

– To generate the wire deformation animation for each atomic bending operation, we uniformly perform linear interpolation over a specific time period. This interpolation is carried out between the *pre-bending wire shape* and the *post-bending wire shape*. The post-bending wire shape corresponds to the target bending segment, while the pre-bending wire shape represents the wire's configuration prior to applying the bending operations. Specifically, for the bend operation, the initial bending angle is set to zero; for the curve operation, the circular segment initially exists as a straight line segment.

– To generate the hand-gesture animations for each atomic bending operation, we meticulously set the positions of two 3D hand models. This process can be divided into two aspects: 1) For the bend operation, we place the two hand models on the two adjacent line segments connected by the bending point, at a distance of 1/4 of the length of the line segment from the bending point. 2) For the curve operation, we position the right hand models along the bending point throughout the animation. For the left hand, when making the first 5 cm of the segment, it remains at the beginning of the segment. Afterwards, it is positioned 5 cm away from the right hand.
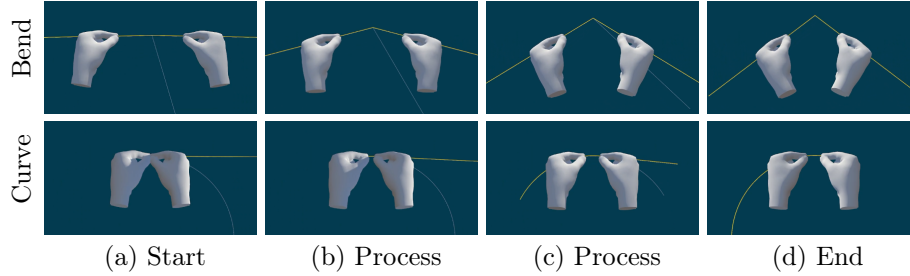

(a) Start   (b) Process   (c) Process   (d) End

Fig. 8. Visualization of our wire deformation animation and hand-gesture animations. For the wire deformation animation, we uniformly perform linear interpolation over a specific time period.

As illustrated in Figure 8, these operation-wise animations offers clear, actionable feedback, enabling novices to follow complex fabrication with minimal ambiguity and difficulties. Additionally, the generated 3D wire and hand-gesture are with identical scale to the physical setting, where the length of the wire precisely corresponds to its real-world counterpart, ensuring accurate guidance, and the size of demonstrated hand's model is approximated to the real setting.

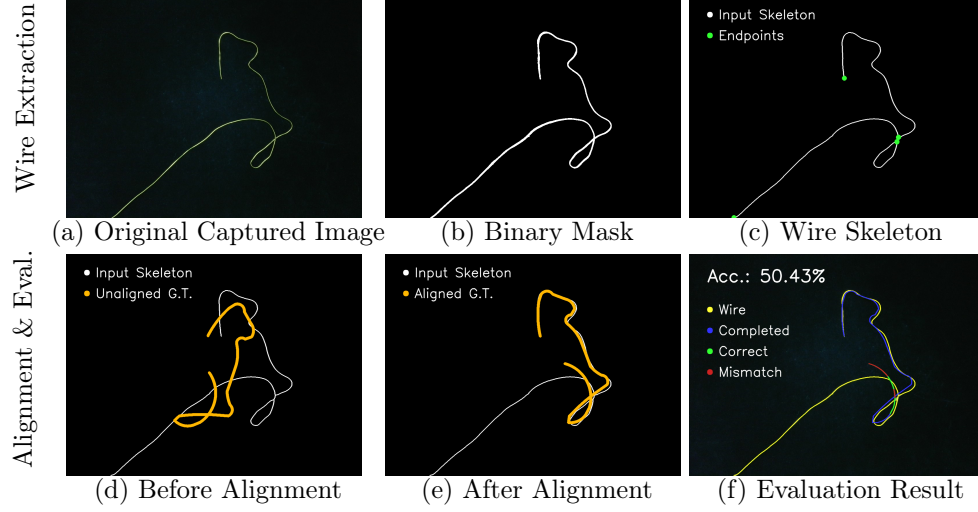## 5.4   Module 3: Real-Time Error Checker

Fig. 9. Illustrations of the processes of our error checker. After capturing the image of the user's progress (a), we first pre-process the image to obtain a binary mask (b), and perform skeletonization to obtain a wire skeleton (c). In the meanwhile, we find all endpoints and intersections (marked as green points in (c)) of the wire skeleton. These points will be used in the following alignment process (d) - (e) to reduce the searching space, thus reducing the computational burden and increase robustness. The alignment process is shown in (d) - (e), where the ground truth are represented as orange curves. After evaluation (f), we provide users with the accuracy of current progress. The user's wire are marked as yellow curves, the completed and accurate (correct) ground-truth are marked as blue and green curves, while the inaccurate (mismatched) parts are highlighted as red curves.

This module features a real-time error checker to evaluate the user's progress, which captures the real-time sequence of images by a photographic apparatus, and compares it to the target line-circular segments S^{final}. Based on the accuracy assessment, it decides if the user can proceed to the next step. Moreover, the checker highlights inaccuracies in the wire with visual feedback, allowing users to quickly identify and rectify errors. This real-time functionality maintains fabrication accuracy while offering intuitive guidance for corrections.

As depicted in Figure 9, when provided with a captured image as input, we employ the following processing pipeline:

Green-blue Region Detection. Recall that users can interactively skip to the next step, even when the current wire product fails to meet the required accuracy threshold. This functionality is enabled by using a printed green-blue cardboard (see Figure 10. When the user intend to skip to next coarse-level bending

segment, they put the cardboard under the photographic apparatus. For each capturing image captured, we detect the green and blue pixels. Once the proportion of these pixels reaches a predefined level, the process will automatically proceed to the next step .

Wire's Skeleton Extraction. This step aims to extract the wire's skeleton from the input image (Figure 9 (a)) with two key steps: 1) first obtain a binary mask with a image pre-processing stage (Figure 9 (b)), including performing gaussian blur to remove small noises, threshold segmentation to strip the wire area, removing connected components with area less than a threshold for further denoising, and binarization; 2) apply Zhang and Suen [47]'s method on the cleaned binary mask to obtain the wire skeleton (Figure 9 (c)). Using a convolution-based neighborhood counting method, we extract all endpoints (degree = 1) and intersection points (degree $\geq$ 3) from the resulting skeleton. These points are then used in the subsequent alignment process.

Optimization-based wire alignment. To match the extracted wire shape with the ground-truth template, we need to align these two shapes (Figure 9 (d)). This task is a classical *rigid registration* problem [1], to minimize the total distance between a transformed ground-truth point set and the extracted input point set. To reduce the computational burden and increase the robustness against to local minima, we propose a key empirical finding: *In nearly all real-world scenarios, the starting point of the fabricated wire shape should closely match that of the ground-truth shape.* Based on this insight, we fix the translation by aligning a chosen input endpoint with the ground-truth starting point, which yields a 1D scalar minimization problem over the rotation angle. To efficiently and robustly solve the 1-DoF optimization problem, we employ a two-stage optimization strategy:

- Coarse Stage: We conduct a grid-search over evenly spaced candidate angles to find a promising initial rotation.
- Fine Stage: A bounded scalar minimization problem is initialized around the best coarse candidate for fine-tuning the alignment, and then optimized using Brent [5]'s method.

For all of these endpoints and intersection points extracting from the wire skeleton, we will try to match it to the endpoint of the ground-truth shape by the above 1-DOF optimization. Then output the one with the minimal matching error, as shown in Figure 9 (e). The above approach enables us to achieve real-time, accurate geometric alignment between the input skeleton and the ground-truth shape.

Wire accuracy evaluation. For each ground-truth point, we query its Euclidean distance to the nearest input skeleton point using a *KD-tree* based nearest point query algorithm. Points exceeding a mismatch threshold are labeled as **incorrect**, which are highlighted in red colors, as shown in Figure 9 (f).

5.5   Hardware and Software

In this section, we meticulously elaborate on our hardware and software configurations, encompassing the parameter settings of the three modules.

Software Setups. Our wire decomposition module is developed using C++ and relies on the following third-party libraries: CGAL [30], libhgp [48], libigl [20], Eigen [17] and gco-v3.0 [34] for geometric computations and graph-cut optimization. In the point sequence P, there is a spacing of 1 cm between each two adjacent points. In *Graph-Cut-Based Segment Fitting*, we set the fitting error threshold $\varepsilon = 0.6$, and set the loss weights $\lambda_1 = 30$, $\lambda_2 = 0.2$, $\lambda_3 = 50$.

Our animated visualization module is developed using Unity Engine [33]. Our real-time error checker module is developed using Python, with the following third-party libraries: OpenCV [4] for image capturing and processing, scikit-image [36] for wire skeletonization, SciPy [35] for the scalar optimizer and KD-tree based nearest point query. The resolution of images captured in the checker is set to 1024×768. The proportion of green-blue pixels required as a threshold for skipping to the next step is setting to $80000/(1024 \times 768)$.

(a) Experimental Setup   (b) Scenario: Operating   (c) Scenario: Checking
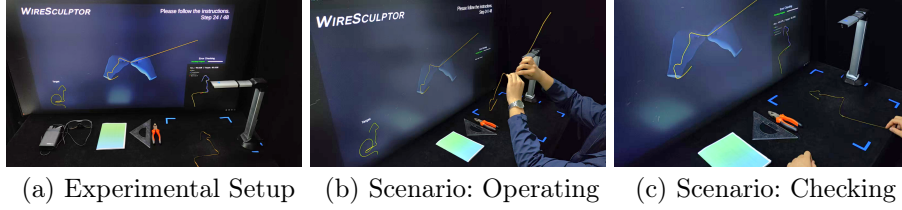
Fig. 10.   An overview of our WireSculptor. (a) Experimental setup. Our system is set in a well-lit room with a 65-inch monitor and a high-speed photographic apparatus. (b) The scenario where the user performs a bending operation, following the animated visualization. (c) The scenario where the user checks the progress. The user puts the wire under the photographic apparatus, and the checker provides real-time accuracy calculation and intuitive feedback.

Hardware Setups. Figure 10 presents the hardware setups of our system. We set our system in a well-lit room with a monitor of 65 inches, and the high-speed photographic apparatus capture the image with the resolution of 768×1024. We test our program on a PC with an Intel Core i7-14700F CPU operating at 5.3 GHz and 64 GB memory. In experiments, our checker can run at a speed of approximately 12 fps and achieve real-time checking.

6   Results and Discussions

We assess the effectiveness and practicality of WireSculptor by comparing it with alternative methods and conducting an ablation study to analyze the necessity of each system module.

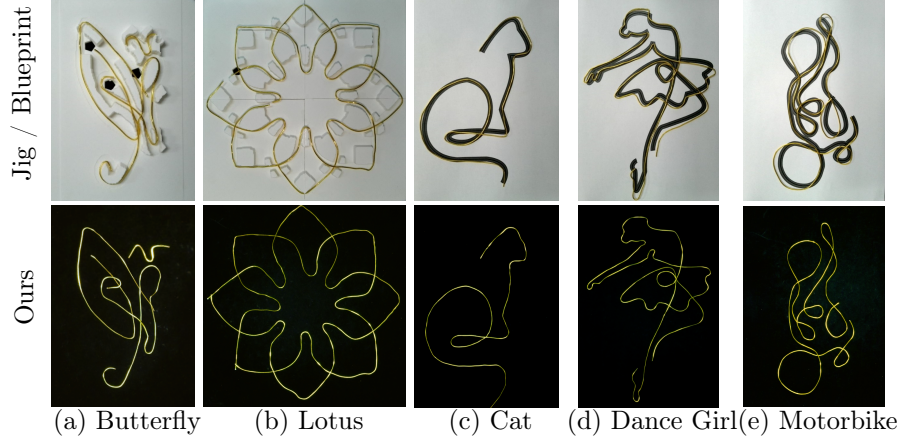## 6.1   Comparative Evaluation

Fig. 11. Fabrication results of the comparative experiment: The first row shows the results of the two alternative approaches (jig and blueprint based methods), while the second row presents the results of our method. From left to right, the sculptures are a butterfly, a lotus, a cat, a dance girl, and a motorbike.

We conducted a user study in a controlled laboratory setting to assess how effectively participants could bend sculptures using our method compared to two alternative approaches: a **blueprint-based manual bending** method and a **physical-model fabrication** method [19]. In the previous approach, users fabricate sculptures by following a paper-printed design. In the latter approach, it provides physical jigs by extruding support walls from 2D jewelry drawings to guide wire wrapping operations [19]. Figure 11 shows the fabrication results of this comparative experiment.

Stimuli. We selected seven wire sculptures from [19,41], encompassing simple shapes like lotus flowers and cats, as well as more complex forms such as human figures and motorbikes. These stimuli were chosen to embody a diverse range of bending challenges in terms of shape complexity and structural detail.

Participants. We recruited 18 participants without any prior wire sculpting experience, consisting of 13 males and 5 females, aged between 19 and 25 years old. During the experiment, participants were seated roughly 60 cm from a 65-inch monitor in a well-lit room. After completing the study, each participant was compensated with a reward of $10.32 per hour for their participation.

Task. Each participant was asked to bend $5 \sim 7$ wire sculptures by following the instructions provided by our method as well as the two alternative approaches.

All trials were presented in a randomized order to each participant to mitigate ordering effects. For each sculpture, we recorded the total time the participant spent on the bending process (termed "fabrication time") and, after the experiment, measured the modified Hausdorff distance [9] (MHD) between the user-bent sculpture and the original design (termed "shape accuracy"). In detail, given two point sets A, B, the MHD between them $H(A, B)$ is defined as:

$$H(A, B) = \max(h(A, B), h(B, A)), \tag{6}$$

where

$$h(A, B) = \frac{1}{|A|} \sum_{a \in A} \min_{b \in B} d(a, b), \tag{7}$$

and $|A|$ denotes the number of points in A, $d(a, b)$ denotes the Euclidean distance between point a and b.

Procedure. Our experiment consisted of three main steps: 1) a training session to introduce the task, consisting of one practice trial; 2) the main experiment; and 3) a short post-experiment interview to help analyze the results. During the main experiment, each participant was presented with $5 \sim 7$ wire designs, along with instructions indicating which method to use. Fabrication time was recorded for each design. On average, participants took approximately 39.6 minutes to complete the main experiment (min: 11.4 minutes, max: 66.6 minutes).

Table 2. Quantitative comparison of fabrication methods. MHD: mean Hausdorff distance [9]. The lower the better. Compared with both methods, our workflow shows advantages for novices in accuracy, within an acceptable time trade-off. Regarding the third component of butterfly, it's an antenna of a butterfly, which is of length 67 mm. Since our error checker allows error tolerance, the closed-loop will complete before the participant finishes fabricating, thus resulting in a poor fabrication quality. However, such scenario of "fabricating tiny components" is unlikely to occur in real-world fabrication.

MHD [9] ↓	Comp. 1	Butterfly Comp. 2	Comp. 3	Lotus	Cat	Dance Girl	Motorbike
Jig [19]	1.835	1.662	1.678	2.567	\	\	\
Blueprint	\	\	\	\	2.064	2.765	2.548
Ours	1.528	1.889	2.262	2.296	1.835	2.404	2.625

Time ↓	Comp. 1	Butterfly Comp. 2	Comp. 3	Lotus	Cat	Dance Girl	Motorbike
Jig [19]	115	179	99	253	\	\	\
Blueprint	\	\	\	\	264	613	454
Ours	174	361	68	593	468	1115	1124

Results. We collected 105 valid results from the experiments, summarized in Table 2. As shown in the table, most participants were able to bend sculptures with higher accuracy when guided by our method compared to the alternative approaches. The time increase observed with our method is, we believe, a reasonable and acceptable trade-off. While our visual guidance system may require more fabrication time due to user interaction with the error checker and the need to watch animations before each bending step, this added duration is offset by the benefits it brings. In particular, the system's real-time feedback, error correction, and step-by-step instructions significantly reduce user uncertainty and prevent cumulative mistakes—factors that are especially important for novice users. We argue that the increased time cost reflects a more deliberate and informed fabrication process, rather than inefficiency. Most importantly, participants generally expressed a positive attitude in our post-experiment interview, which will be discussed in the following section.

6.2   Post-Experiment Interview

To complement the quantitative evaluation, we conducted a post-experiment interview with all participants. Our interview was carried out in the form of a structured questionnaire, comprising nine questions that investigated participants' subjective experience with the three bending assistance tools. Specifically, the questionnaire asked the following:

1. Compared to our WireSculptor workflow, did you find the blueprint/jig method easier or more comfortable to use?
2. Why did you find your preferred method more effortless or comfortable?
3. After trying all three methods, what advantages do you think our workflow offers?
4. If you could choose one method to continue using, which one would you choose and why?
5. Do you think blueprint-based bending guidance is suitable for beginners? Why or why not?
6. Did you encounter any difficulties when using the blueprint method (e.g., ambiguity at intersections)?
7. Do you think the jig method is suitable for beginners?
8. How would you rate our workflow? (Scale: –5 to 5, higher is better)
9. Do you have any comments or suggestions for our workflow?

We have collected 9 valid responses from participants. The responses provide insights into the subjective experience and usability of these three bending assistance tools.

Ease of Use and Intuitiveness. Most participants (6 of 9 valid interview results) found our system significantly more intuitive and less physically demanding. As one participant noted, *"WireSculptor tells me how far I should bend in each step. It feels like it's bending with me."* Another commented that *"WireSculptor*

gives feedback and shows what I did wrong, helping me fix it before moving on." Compared to the paper blueprint, which several participants described as *"confusing at wire intersections"* and *"lacking interaction"*, our system's dynamic, real-time feedback was repeatedly cited as a key advantage. One participant emphasized that *"blueprint-based designs are hard to follow when wires overlap, but the WireSculptor always shows what to do next."*

Effectiveness for Novice Users. A notable theme is how well our method supported novice users. Nearly all participants (8 of 9 valid interview results) believed the visual guidance tool was more suitable for novices than the alternatives (e.g., blueprint and jig). As one participant put it, *"each step gave me feedback and made me confident I could finish the piece."* In contrast, the blueprint and jig-based methods were often described as requiring experience or trial-and-error. One participant noted that *"with the 3D jig, it was hard to know where the wire should go next."*

Engagement and Satisfaction. Participants also found our system more engaging and enjoyable. Several referred to the visual guidance tool as *"more fun"* and *"more interactive"* than the alternatives. One participant praised its ability to guide without breaking immersion: *"It's like the system is folding with me, step by step."* In contrast, some participants mentioned that with blueprint or jig-based methods, *"you often finish the whole shape before realizing something went wrong."*

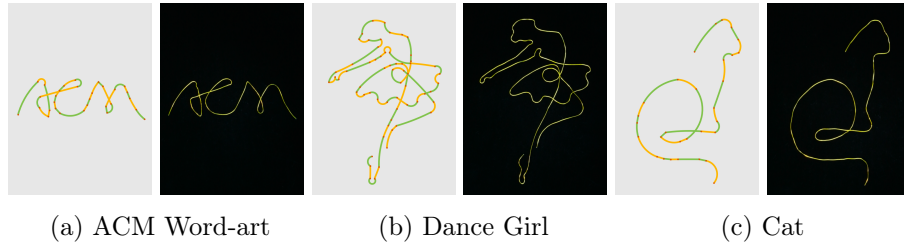(a) ACM Word-art   (b) Dance Girl   (c) Cat

Fig. 12. Illustrations of the application of our workflow in wire sculpture fabrication for novices. Whether the design is simple or complex (the first, third, fifth columns), with our workflow, novices are capable of fabricating nice-looking corresponding wire sculpture (the second, fourth, sixth columns).

Rating and Feedback. On a -5 to 5 rating scale (the higher the better), our system received an average score of **3.78**, with most participants (7 of 9) assigning it a 4 or 5. Participants appreciated its precision and interactivity, while also suggesting minor usability improvements. For instance, a few participants noted that *"placing the screen closer to the wire could reduce head movement,"* and that *"being able to replay a bending step would be helpful when catching up."*

These qualitative results reinforce our experimental results: our system not only improves bending accuracy, but also transforms the fabrication experience into a guided, confident, and even enjoyable process, particularly for novices. The integration of animated visualization, real-time checking and interactive feedback distinguishes our system as a more usable and empowering tool for wire sculpting.

7   Applications

We demonstrate that our workflow is flexible to support diverse creative use cases. In this section, we present two key application scenarios.

7.1   Wire Sculpture Fabrication for Novices

Our workflow enables novice users to create aesthetically pleasing and structurally sound wire sculptures with minimal prior experience. We showcase three examples in Figure 12: a stylized ACM word-art, a dance girl figure, and a sitting cat. Throughout these tasks, novice users benefited from the WireSculptor's coarse-to-fine segmentation of steps, allowing them to focus on one bending operation at a time without being overwhelmed. The integrated error checker provided instant feedback, helping novice users identify and correct errors early before they propagated. By removing much of the guesswork traditionally associated with the craft, our system empowers novice users to achieve professional-looking results with minimal frustration.

7.2   Innovative Educational Hand-Crafting for Children

Beyond regular sculpture fabrication tasks, our workflow also serves as an educational tool for children to engage in hand-crafting with the support of their parents or educators. In this setting, children sketch their desired shapes, and parents then handle the physical bending with the assistance of our interactive animation and visual feedback tools. This collaborative process allows children to participate in both the design and evaluation loop, encouraging creativity and hands-on learning. Figure 13 showcases three sample outcomes produced through child-parent collaboration. Each of them captures the child's original design while maintaining physical fidelity.

8   Conclusion

In this paper, we present *WireSculptor*, an innovative interactive workflow that enables novices to fabricate wire sculptures through a guided, step-by-step process. Our workflow combines the intuitiveness of human-in-the-loop hand crafting with the precision of visual feedback and error checking. We designed the system around three core modules: wire decomposition with a formative study,
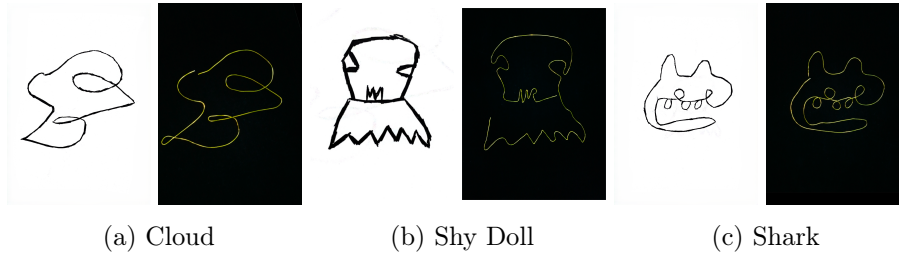
(a) Cloud   (b) Shy Doll   (c) Shark

Fig. 13. Illustrations of the application of our workflow in innovative educational hand-crafting for children. After children sketching their desired shapes (the first, third, fifth columns), adults can assist in transforming the shapes into wire sculptures (the second, fourth, sixth columns).

interactive animated visualization, and a real-time error checker. Through user experiments, we validated the effectiveness of our workflow in improving fabrication accuracy and accessibility for novices.

Limitations Our interactive guided animations, being screen-displayed, suffer from the drawback of not being viewable from all directions. Also, in our fabrication, we didn't account for wire characteristics like thickness and hardness, beyond just its length, and future studies could incorporate these. Methodologically, we're restricted to single, non-self-closing wires, topologically limiting the artworks we can guide, so introducing multiple wires and self-closing wires is a future prospect. In terms of time cost, our method consumes excessive time in the fabrication of many shapes, with the analysis revealing the following reasons. Firstly, our system involves the use of multiple operational modules, like animated visualization module and real-time error checker module, resulting in a steeper learning curve compared to other methods. Secondly, our operation module and visualization module are separate entities, requiring users to constantly contrast both modules during tasks, which incurs a time overhead for this comparison process. Finally, the animation playback and demonstration process incurs a time overhead.

Future Work We plan to expand the 3D wire sculpture fabrication, and the assembly process of multi-wires. To enhance user freedom, we aim to enable the system to dynamically plan operations in response to users' real-time bending actions as their skills develop. We also intend to integrate AI techniques, such as large language models (LLMs), to help generate dynamic bending guidance for wire sculpture fabrication. Furthermore, it would be fascinating to incorporate mixed-reality devices into our system. Using mixed-reality devices can integrate our operation module and visualization module into a unified system, facilitating user learning and operation, thereby reducing the system's time overhead. To achieve this, we need to solve the problem of real-time error detection based on 3D wire reconstruction. Another promising direction is to expand the application domains of WireSculptor. For example, we could investigate its use in creating

more complex 3D wire-frame structures for architectural models or in the field of industrial prototyping. And the other direction is to enhance system efficiency. Designing more flexible control strategies such as introducing an adaptive mode that reduces animation playback time and decreases inspection frequency as users become more proficient can enhance system efficiency and reduce time consumption.

Disclosure of Interests. The authors have no competing interests to declare that are relevant to the content of this article.

References

1. Ashburner, J., Friston, K.J.: Rigid body registration. Statistical parametric mapping: The analysis of functional brain images pp. 49–62 (2007)
2. Baraldo, A., Bascetta, L., Caprotti, F., Chourasiya, S., Ferretti, G., Ponti, A., Sakcak, B.: Automatic computation of bending sequences for wire bending machines. International Journal of Computer Integrated Manufacturing **35**(12), 1335–1351 (2022)
3. Bhundiya, H.G., Cordero, Z.C.: Bend-forming: A cnc deformation process for fabricating 3d wireframe structures. Additive Manufacturing Letters **6**, 100146 (2023)
4. Bradski, G.: The OpenCV Library. Dr. Dobb's Journal of Software Tools (2000)
5. Brent, R.P.: Algorithms for minimization without derivatives. Courier Corporation (2013)
6. Cheng, L., Jia, H., Yu, L., Wu, Y., Ye, S., Deng, D., Zhang, H., Xie, X., Wu, Y.: Viscourt: In-situ guidance for interactive tactic training in mixed reality. In: Proceedings of the 37th Annual ACM Symposium on User Interface Software and Technology. pp. 1–14 (2024)
7. Cohen-Or, D., Greif, C., Ju, T., Mitra, N.J., Shamir, A., Sorkine-Hornung, O., Zhang, H.R.: A Sampler of Useful Computational Tools for Applied Geometry, Computer Graphics, and Image Processing. A. K. Peters, Ltd., USA, 1st edn. (2015)
8. Dong, J., Xia, Z., Zhao, Q., Zhao, N.: Human–machine integration based augmented reality assisted wire-bending training system for orthodontics. Virtual Reality **27**(2), 627–636 (2023)
9. Dubuisson, M.P., Jain, A.: A modified hausdorff distance for object matching. In: Proceedings of 12th International Conference on Pattern Recognition. vol. 1, pp. 566–568 vol.1 (1994). https://doi.org/10.1109/ICPR.1994.576361
10. Etsy: Wire 'grateful' Sign, Handmade Wire Words, Names, Phrases, Quotes, Lyrics, Metal Wall Art, Cursive Lettering - Etsy UK | Grateful signs, Hanging signs, Handmade wire — kr.pinterest.com. https://kr.pinterest.com/pin/1127659194200817649/ (2025), [Accessed 01-05-2025]

11. Fang, W., Zhang, T., Chen, L., Hu, H.: A survey on hololens ar in support of human-centric intelligent manufacturing. Journal of Intelligent Manufacturing **36**(1), 35–59 (2025)

12. Feng, S., Liu, B., Berman, O., Haraldsson, H., Roumen, T., et al.: Y-ar: A mixed reality cad tool for 3d wire bending. arXiv preprint arXiv:2410.23540 (2024)

13. Firoozabadi, R., Kramer, P.A., Benirschke, S.K.: Kirschner wire bending. Journal of Orthopaedic Trauma **27**(11), e260–e263 (2013)

14. France, M.M., Shallit, J.O.: Wire bending. Journal of Combinatorial Theory, Series A **50**(1), 1–23 (1989)

15. Garg, A., Sageman-Furnas, A.O., Deng, B., Yue, Y., Grinspun, E., Pauly, M., Wardetzky, M.: Wire mesh design. ACM Transactions on Graphics **33**(4) (2014)

16. GreccoSimone: família wire sculpture Simone Grecco | Esculturas em arame, Esculturas, Artistas — kr.pinterest.com. https://kr.pinterest.com/pin/844493664835104/ (2025), [Accessed 01-05-2025]

17. Guennebaud, G., Jacob, B., et al.: Eigen v3. http://eigen.tuxfamily.org (2010)

18. Gupta, A., Fox, D., Curless, B., Cohen, M.: Duplotrack: a real-time system for authoring and guiding duplo block assembly. In: Proceedings of the 25th annual ACM symposium on User interface software and technology. pp. 389–402 (2012)

19. Iarussi, E., Li, W., Bousseau, A.: Wrapit: computer-assisted crafting of wire wrapped jewelry. ACM Transactions on Graphics (TOG) **34**(6), 1–8 (2015)

20. Jacobson, A., Panozzo, D., et al.: libigl: A simple C++ geometry processing library (2018), https://libigl.github.io/

21. Lee, W., Prasad, R., Je, S., Kim, Y., Oakley, I., Ashbrook, D., Bianchi, A.: Virtualwire: Supporting rapid prototyping with instant reconfigurations of wires in breadboarded circuits. In: Proceedings of the Fifteenth International Conference on Tangible, Embedded, and Embodied Interaction. pp. 1–12 (2021)

22. Li, W.: Pen2vr: A smart pen tool interface for wire art design in vr (2021)

23. Lira, W., Fu, C.W., Zhang, H.: Fabricable eulerian wires for 3d shape abstraction. ACM Transactions on Graphics (TOG) **37**(6), 1–13 (2018)

24. Liu, M., Zhang, Y., Bai, J., Cao, Y., Alperovich, J.M., Ramani, K.: Wirefab: mix-dimensional modeling and fabrication for 3d mesh models pp. 965–976 (2017)

25. Liu, R., Wan, W., Harada, K.: Tamp for 3d curving—a low-payload robot arm works aside a bending machine to curve high-stiffness metal wires. IEEE Transactions on Automation Science and Engineering (2023)

26. Miguel, E., Lepoutre, M., Bickel, B.: Computational design of stable planar-rod structures. ACM Transactions on Graphics (TOG) **35**(4), 1–11 (2016)

27. Ogden, J.M.: Classical gold wire: some aspects of its manufacture and use. Jewellery studies **5**, 95–105 (1991)

28. Osti, F., de Amicis, R., Sanchez, C.A., Tilt, A.B., Prather, E., Liverani, A.: A vr training system for learning and skills development for construction workers. Virtual Reality **25**, 523–538 (2021)

29. Sun, L., Li, J., Chen, Y., Yang, Y., Yu, Z., Luo, D., Gu, J., Yao, L., Tao, Y., Wang, G.: Flextruss: A computational threading method for multi-material, multi-form and multi-use prototyping. In: Proceedings of the 2021 CHI Conference on Human Factors in Computing Systems. pp. 1–12 (2021)

30. The CGAL Project: CGAL User and Reference Manual. CGAL Editorial Board, 6.0.1 edn. (2024), https://doc.cgal.org/6.0.1/Manual/packages.html

31. Tojo, K., Shamir, A., Bickel, B., Umetani, N.: Fabricable 3d wire art. In: ACM SIGGRAPH 2024 Conference Proceedings. SIGGRAPH '24 (2024). https://doi.org/10.1145/3641519.3657453

32. Torres, C., Li, W., Paulos, E.: Proxyprint: Supporting crafting practice through physical computational proxies. In: Proceedings of the 2016 ACM Conference on Designing Interactive Systems. pp. 158–169 (2016)
33. Unity Technologies: Unity 6.0 (2025), https://unity.com/releases, accessed: 2025-03-30
34. Veksler, O., Delong, A.: gco-v3.0. https://github.com/nsubtil/gco-v3.0 (2015)
35. Virtanen, P., Gommers, R., Oliphant, T.E., Haberland, M., Reddy, T., Cournapeau, D., Burovski, E., Peterson, P., Weckesser, W., Bright, J., van der Walt, S.J., Brett, M., Wilson, J., Millman, K.J., Mayorov, N., Nelson, A.R.J., Jones, E., Kern, R., Larson, E., Carey, C.J., Polat, İ., Feng, Y., Moore, E.W., VanderPlas, J., Laxalde, D., Perktold, J., Cimrman, R., Henriksen, I., Quintero, E.A., Harris, C.R., Archibald, A.M., Ribeiro, A.H., Pedregosa, F., van Mulbregt, P., SciPy 1.0 Contributors: SciPy 1.0: Fundamental Algorithms for Scientific Computing in Python. Nature Methods **17**, 261–272 (2020). https://doi.org/10.1038/s41592-019-0686-2
36. van der Walt, S., Schönberger, J.L., Nunez-Iglesias, J., Boulogne, F., Warner, J.D., Yager, N., Gouillart, E., Yu, T., the scikit-image contributors: scikit-image: image processing in Python. PeerJ **2**, e453 (6 2014). https://doi.org/10.7717/peerj.453, https://doi.org/10.7717/peerj.453
37. Wang, B., Wang, G., Sharf, A., Li, Y., Zhong, F., Qin, X., CohenOr, D., Chen, B.: Active assembly guidance with online video parsing. In: 2018 IEEE Conference on Virtual Reality and 3D User Interfaces (VR). pp. 459–466. IEEE (2018)
38. Wang, G., Qin, F., Liu, H., Tao, Y., Zhang, Y., Zhang, Y.J., Yao, L.: Morphingcircuit: An integrated design, simulation, and fabrication workflow for self-morphing electronics. Proceedings of the ACM on Interactive, Mobile, Wearable and Ubiquitous Technologies **4**(4), 1–26 (2020)
39. Wang, Y., Yang, X., Fukusato, T., Igarashi, T.: Computational design and fabrication of 3d wire bending art pp. 1–2 (2019)
40. Wikipedia contributors: Wire sculpture — Wikipedia, the free encyclopedia. https://en.wikipedia.org/w/index.php?title=Wire_sculpture&oldid=1272801587 (2025), [Online; accessed 27-March-2025]
41. Wu, Q., Zhang, Z., Yan, X., Zhong, F., Zhu, Y., Lu, X., Xue, R., Li, R., Tu, C., Zhao, H.: Tune-it: Optimizing wire reconfiguration for sculpture manufacturing. In: SIGGRAPH Asia 2024 Conference Papers. SA '24, Association for Computing Machinery, New York, NY, USA (2024). https://doi.org/10.1145/3680528.3687588, https://doi.org/10.1145/3680528.3687588
42. Xu, H., Knoop, E., Coros, S., Bächer, M.: Bend-it: design and fabrication of kinetic wire characters. ACM Transactions on Graphics (TOG) **37**(6), 1–15 (2018)
43. Yang, Z., Xu, P., Fu, H., Huang, H.: Wireroom: model-guided explorative design of abstract wire art. ACM Transactions on Graphics (TOG) **40**(4), 1–13 (2021)
44. Yu, J., Kuruppu, S., Fernando, B., Perera, P.B., Sugiura, Y., Subramanian, S., Withana, A.: Irontex: Using ironable 3d printed objects to fabricate and prototype customizable interactive textiles. Proceedings of the ACM on Interactive, Mobile, Wearable and Ubiquitous Technologies **8**(3), 1–26 (2024)
45. Yu, M., Ye, Z., Liu, Y.J., He, Y., Wang, C.C.: Lineup: Computing chain-based physical transformation. ACM Transactions on Graphics (TOG) **38**(1), 1–16 (2019)
46. Yue, Y.T., Zhang, X., Yang, Y., Ren, G., Choi, Y.K., Wang, W.: Wiredraw: 3d wire sculpturing guided with mixed reality. In: Proceedings of the 2017 CHI Conference on Human Factors in Computing Systems. pp. 3693–3704 (2017)
47. Zhang, T.Y., Suen, C.Y.: A fast parallel algorithm for thinning digital patterns. Commun. ACM **27**(3), 236–239 (Mar 1984). https://doi.org/10.1145/357994.358023, https://doi.org/10.1145/357994.358023

48. Zhao, H.: libhgp. Zhao, Haisen (2 2024), https://github.com/haisenzhao/libhgp